



Short communication

Evaluation of 5 kW proton exchange membrane fuel cell stack operated at 95 °C under ambient pressure

Zhengkai Tu^a, Haining Zhang^{a,b,*}, Zhiping Luo^{a,b}, Jing Liu^c, Zhongmin Wan^{c,**}, Mu Pan^{a,b}

^a State Key Laboratory of Advanced Technology for Materials Synthesis and Processing, Wuhan University of Technology, Wuhan 430070, China

^b Key Laboratory of Fuel Cell Technology of Hubei Province, Wuhan University of Technology, Wuhan 430070, China

^c School of Physics, Hunan Institute of Science and Technology, Yueyang, Hunan 414006, PR China

HIGHLIGHTS

- PEMFC based on short side chain perfluorinated ionomer composite membranes are prepared.
- Cell voltage at 800 mA cm⁻² of PEMFC reaches 0.61 V at 95 °C under 40% RH and ambient pressure.
- The temperature of inlet gases affects the stack performance.

ARTICLE INFO

Article history:

Received 9 July 2012

Received in revised form

28 August 2012

Accepted 29 August 2012

Available online 12 September 2012

Keywords:

Proton exchange membrane fuel cell

Short side chain

Composite membrane

Elevated temperature

Reduced humidity

ABSTRACT

Composite membranes containing ePTFE matrix and short side chain perfluorinated ionomers are introduced as electrolytes for proton exchange membrane fuel cell applications. The output voltage at 800 mA cm⁻² for single cell using composite membrane as electrolyte reaches 0.61 V at 95 °C under 40% relative humidity whereas it is only 0.41 V for cell assembled from pristine short side chain perfluorinated sulfonated membrane at the same condition. The performance of fuel cell stack using composite membrane as electrolyte in kilowatts ranges has been experimentally investigated at 95 °C under ambient pressure. With the increase in the inlet gas temperature, the performance of the stack is enhanced. The non-monotonic behavior in instantaneous average voltage of single cells in the stack has been observed and the peak value is appeared at the stack temperature of 90 °C. The observed water accumulation phenomena suggest that the decrease in stack performance above 90 °C is attributed to the lack of water in the system. The results observed in this study demonstrate that the composite membrane has the potential operating at 95 °C under reduced relative humidity to 40%, which is a suitable operating condition for fuel cell vehicle applications.

© 2012 Elsevier B.V. All rights reserved.

1. Introduction

As one of the promising clean energy sources, proton exchange membrane fuel cell (PEMFC), also known as polymer electrolyte membrane fuel cell, has attracted increasing attention because of its high power density and wide range of applicability including automotive and stationary applications [1,2]. As restricted by proton conduction and current formation mechanisms, operating temperature below 80 °C and high humidification level are generally required for the state of the art of PEMFC. The thus-applied

large radiator and humidification sub-system can not only decrease the power density, but also increase the cost of PEMFC, which is a major barrier limiting its further widespread applications [3,4]. The increase in operating temperature of PEMFC can effectively decrease the size of the radiator because of the simplified heat management [5]. In addition, the increased operation temperature can improve the quality of generated heat, making the application of PEMFC in combined heat and power (CHP) systems more practically possible [6–8].

The well-developed high temperature PEMFC stacks are those using polybenzimidazole doped membranes with phosphoric acid as electrolytes, having operation temperature typically in the range of 150–200 °C [9]. Sanderson et al., from FuelCell Energy Inc. in the US reported series assembled PEMFC stacks using phosphoric acid doped PBI membranes as electrolytes, with rated power from 2 kW to 15 kW [10]. However, technical challenges of PEMFC using phosphoric acid doped PBI membranes including relatively low

* Corresponding author. State Key Laboratory of Advanced Technology for Materials Synthesis and Processing, Wuhan University of Technology, Wuhan 430070, China. Tel.: +86 27 87651839 8611; fax: +86 27 87879468.

** Corresponding author. Fax: +86 730 8648870.

E-mail addresses: haining.zhang@whut.edu.cn (H. Zhang), zhongminwan@hotmail.com (Z. Wan).

power density, difficulty of start-up from room temperature, and dramatic degradation after certain operation time (reaching $0.67 \mu\text{V s}^{-1}$ as reported by Pinar et al. [11]) still need to be resolved prior to practical applications.

Recently, short side chain perfluorinated ionomers developed by Solvay Solexis with trademark of Aquion[®] have provided another choice for high temperature electrolytes used in PEMFCs. Compared to the well-known Nafion[®] membranes, membranes made from short side chain perfluorinated ionomers exhibited an improved water retention ability and higher glass transition temperature, making them possible for high temperature PEMFC applications [12–14]. It has been demonstrated that the short stack composed of 6 membrane electrode assemblies (MEAs) with active area of 360 cm^2 using Aquion membranes as electrolytes has appropriate performance in a wide temperature range from ambient to 110°C under increased system pressure of 1.5 bar [15]. However, the increased system pressure could offset the benefit from high temperature. Thus, the operating temperature in short term requirement of PEMFC for automotive applications is set to $90\text{--}95^\circ\text{C}$ based on the state of the art of membrane technology [16].

In this communication, we report the design and assembly of a 5 kW PEMFC stack using composite membranes consisting of short side chain perfluorinated ionomers and ePTFE as electrolytes. The performance of the assembled stack has been evaluated at the operating temperature of 95°C under ambient pressure. In addition, the water accumulation at the outlet of cathode was monitored under different operating conditions.

2. Experimental

The short side chain perfluorinated ionomers with equivalent weight of 890 g mol^{-1} and pristine short side chain perfluorinated sulfonate membrane with thickness of $30 \mu\text{m}$ were received from Huaxia Shenzhou New Material Co. Ltd., China. The chemical structure of the applied ionomers is shown in Fig. 1. Polymer electrolyte composite membranes composed of short side chain perfluorinated ionomers and ePTFE were prepared by following our previous work [17]. The typical thickness of the so-formed composite membrane is about $12.5 \mu\text{m}$. Because of the introduction of non-proton conducting ePTFE matrix, the equivalent of the membrane increased to 1209 g mol^{-1} as determined by titration of ion-exchanged solution [18]. The physical and electrochemical properties of the formed composite membranes were listed in Table 1. The performance of MEA with active area of 25 cm^2 and Pt (Hispec[™] 9100, Johnson Matthew) loading of 0.4 mg cm^{-2} using Nafion ionomers (EW 1100, DuPont) as proton conducting materials in electrode for both anode and cathode at 95°C under different relative humidities were investigated on FCATS G50 (GreenLight In. Co., Canada) with hydrogen and air stoichiometry values of 1.5 and 2.5, respectively.

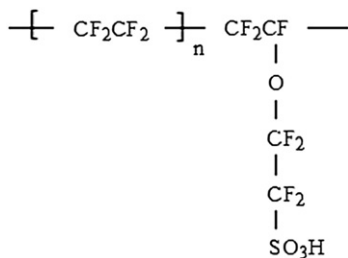


Fig. 1. Chemical structure of the short side chain perfluorinated ionomers used in this study.

Table 1

Physical and electrochemical properties of composite membranes based on short side chain perfluorinated sulfonated ionomers.

PEM thickness (m)	1.0×10^{-5}
EW	1209
Bulk density (g cm^{-3})	1.93
Surface conductivity (S cm^{-2})	48.4
Mechanical strength (MPa)	50.8
Swelling rate (%)	23
Permeability/OCV	0.95
Swelling stress	<0.5
Catalyst layer thickness (m)	1.2×10^{-5}

The MEAs with active area of 200 cm^2 were fabricated using catalyst-coated membrane method as reported previously [19,20]. Loading of Pt electrocatalyst (Hispec[™] 9100, Johnson Matthew) on both anode and cathode is 0.4 mg cm^{-2} . Nafion ionomers were used as proton conducting materials in electrodes. Carbon paper (TGP-060, Toray) hydrophobically treated with PTFE was used as gas diffusion layer and microporous layer (MPL) was brushed in the carbon paper. The treated carbon paper was then pressed on both sides of catalyst-coated membrane. The designed PEMFC stack composed of 75 pairs of graphite plates with special serpentine flow field was assembled under pressure of 1 MPa by connecting each MEA in series between two graphite plate pairs. The reaction gases are in co-flow mode during the cell operation. The cooling channels were designed on the back of each graphite plate and deionized water at pre-set temperature was circulated as coolant to keep almost constant temperature of the stack during polarization investigation. The assembled PEMFC stack is shown in Fig. 2 and geometric properties of the assembled stack are listed in Table 2. Prior to the performance evaluation of the stack, internal and external leakages of reaction gases were tested and the result was found to be acceptable.

The performance tests of the assembled stack were carried on FCATS G500 (GreenLight In. Co., Canada). The maximum testing power of the test station was 12.5 kW. Operational parameters including electronic load, hydrogen and air flux or gas excessive coefficient, dew point temperature, the stack temperature and back-pressure can be controlled precisely with the supplied program. Several additional temperature and pressure sensors were also introduced to the test system to evaluate the variation of such parameters in the stack. The schematic diagram of the modified test system is shown in Fig. 3. The humidification level of

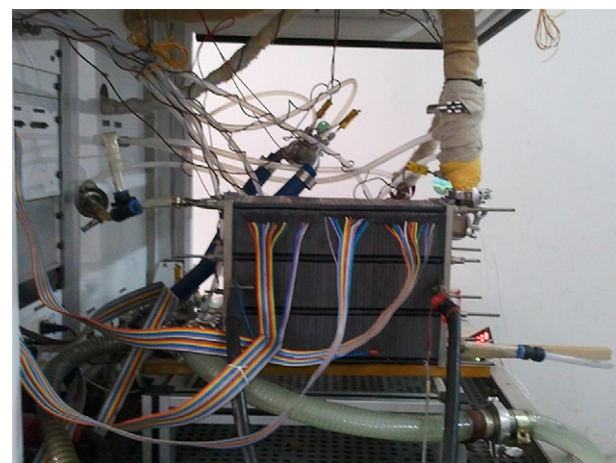


Fig. 2. The 5 kW-class PEM fuel cell stack. Active area of MEA: 200 cm^2 ; 75 cell stack.

Table 2

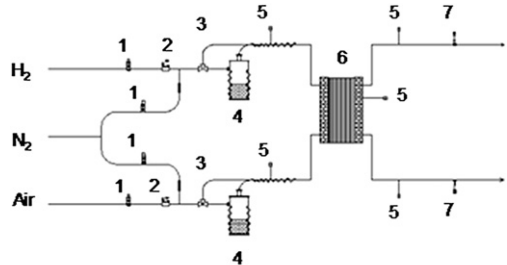
Geometric parameters of the fuel cell stack assembled in this study.

Single cell area of this stack (m^2)	200×10^{-4}
Flow field depth (m)	1.0×10^{-3}
Flow field width (m)	1.0×10^{-3}
Flow field ridge width (m)	1.0×10^{-3}
Gas diffusion layer thickness (m)	2.5×10^{-4}
PEM thickness (m)	1.0×10^{-5}
Catalyst layer thickness (m)	1.2×10^{-5}

the reaction gases was controlled by the inlet temperature of gases passed through the humidifiers (with the same temperature of inlet gas) under ambient pressure. In this study, the cathode gas was humidified for all experiments and both humidified and non-humidified anode gases were applied. For the non-humidified hydrogen operating conditions, the humidifier for hydrogen in the test station was set at "By pass" to make sure that the dry hydrogen was supplied into the stack. During the test process, the polarization curves of each single cell were recorded as well. The hydrogen and air flow rates in this study were set to 200 lpm and 650 lpm, respectively. Unless otherwise stated, the temperature of the stack was kept at 95 °C. To monitor the water accumulation phenomena, a high-speed vision camera (IEEE 1394b, AVT, German) with pixel of 1024 × 768 and shoot speed of 270 frames per second was introduced at the outlet of cathode.

3. Results and discussion

The performance of MEA based on short side chain perfluorinated ionomer composite membrane in this study was first investigated at single cell level with active area of 25 cm^2 before applied to stack assembly. The polarization curves of assembled single cell at 95 °C under various relative humidity were plotted in Fig. 4. As comparison, the polarization curves of the assembled single cell at 65 °C and 100% relative humidity and the cell assembled from pristine membrane at 95 °C and 50% relative humidity were plotted in the same figure. Under 100% relative humidity and ambient pressure, it was observed that the cell voltage slightly decreased from 0.65 V to 0.64 V at current density of 800 mA cm^{-2} with the increase in operating temperature from 65 to 95 °C, attributed to the decreased partial pressure of reaction gases in electrodes with the increase in operating temperature. It can be seen that the cell voltage decreased with the decrease in relative humidity at 95 °C. While the relative humidity decreased from 100% to 40%, about 0.03 V decrease in cell voltage was observed. This decrease in cell voltage with the relative humidity resulted from the dehydration of the membrane and the according increase of the internal resistance. However, it is evident that the cell using composite membrane as electrolyte performs much



1. Pressure controller; 2. Flowmeter; 3. Bypass;
4. Water reservoir; 5. Temperature sensor;
6. Stack; 7. Pressure sensor

Fig. 3. Schematic diagram of the testing system of PEM fuel cell stack.

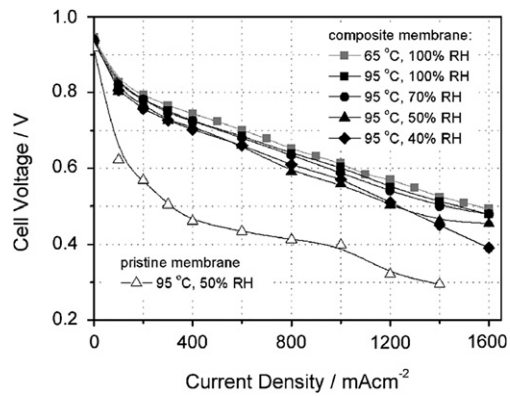


Fig. 4. Polarization curves of MEAs made from composite membrane (solid) and pristine short side chain perfluorinated sulfonated ionomer membrane (open) under different conditions as described in the figure.

better at 95 °C and reduced relative humidity than that using pristine short side chain perfluorinated ionomer membrane as electrolyte. The output voltage of cell using composite membrane as electrolyte at 95 °C and 40% relative humidity reached 0.61 V at 800 mA cm^{-2} that is about 0.2 V higher than the cell assembled from pristine membrane. The less humidity-dependant performance of the cell using composite membrane as electrolyte is attributed to the thinner composite membrane applied (12.5 μm) compared to pristine membrane (30 μm) as the thin membrane can facilitate the water management and the electrochemical reaction generated water at cathode can migrate easily to anode by back diffusion [21]. Accordingly, the back-diffused water can reduce the internal resistance of the cell, leading to improved cell performance at relatively low humidification conditions. Thus, fuel cell using composite membrane as electrolyte has great potential operated under reduced humidification levels and stacks based on composite membrane electrolyte were developed.

Prior to evaluation of the performance, the assembled fuel cell stack was pre-activated with increasing current using both fully humidified cathode and anode gases for about 12 h until stable performance was reached. Polarization curves of the stack at 95 °C under ambient pressure with different humidification conditions were plotted in Fig. 5. The humidification was controlled by the temperature of inlet gases and the values of relative humidity were calculated according to saturated water vapor pressures as approximately 45.6%, 56.0%, and 68.4% for inlet gas temperatures of 75 °C, 80 °C, and 85 °C, respectively. It is evident, that the stack supplied with humidified gas performs better than that supplied with dry anode gas, probably attributed to the decreased membrane resistance with humidified anode gas. When the inlet

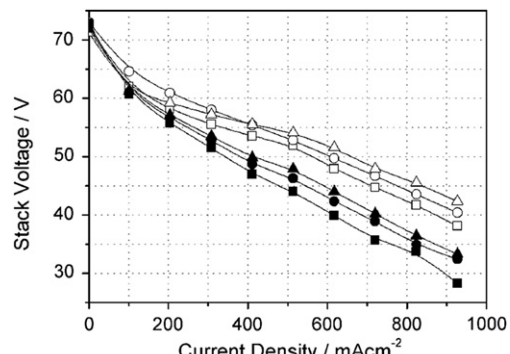


Fig. 5. Polarization curves of assembled stack with the supply of dry hydrogen (solid) and humidified hydrogen (open) under different inlet gas temperatures: 75 °C (square), 80 °C (circle), and 85 °C (triangle).

temperature varied from 75 °C to 85 °C, the output voltage of the stack at 600 mA cm⁻² increased from 47.9 V to 51.5 V with supply of humidified anode gas and it increased from 39.9 V to 44.0 V with supply of dry anode gas. Although the performance of the stack can be enhanced with the increase of the inlet gas temperature, the output voltages are acceptable for the stack supplied with both humidified anode and cathode gases under relatively low inlet gas temperature, i.e. relative humidity reduced down to about 45%. In addition, the average voltage of each cell in the stack was observed to be about 0.64 V at 600 mA cm⁻² at 95 °C and 45.6% relative humidity, which is about 0.02 V lower than that of single cell under similar conditions. This result indicates that the further improvement for assembly process of the stack is required.

The output power of the assembled stack at 95 °C was plotted as a function of current density in Fig. 6 for different inlet gas temperatures. It can be clearly seen that the output power increases with the increase in inlet gas temperature for supply of both humidified and dry anode gas. With the increase of the inlet gas temperature from 75 °C to 85 °C, the output power of the stack at 900 mA cm⁻² increased from 7.10 kW to 7.84 kW for the supply of humidified anode gas and it increased from 5.10 kW to 6.00 kW while the dry anode gas was supplied. When the humidified anode gas was supplied, the increased inlet gas temperature can lead to the increased humidity of the system and the enhanced electrode reaction kinetics, resulting in an improved performance of the stack. For the dry anode gas testing conditions, the increased inlet gas temperature may enhance the electrode reaction kinetics and the back diffusion of water from cathode to anode, leading to the improved performance of stack. However, detailed experiments are required to be carried out to elucidate the temperature effect of inlet gases on the performance of the stack.

Voltage uniformity of each single cell in the stack is of importance for the performance and the potential durability of the stack. Voltage distribution values of each single cell in the stack at 95 °C and 600 mA cm⁻² under different test conditions are displayed in Fig. 7. It can be seen that the fluctuation of voltage distribution for single cells in the stack is more significant supplied with dry anode gas than that supplied with humidified anode gas. This could be attributed to the uneven water distribution in the membrane when the dry anode gas was supplied since the water evaporated relatively fast at the stack temperature of 95 °C. When the humidified anode gas was fed to the stack, the water molecules in the anode gas may balance the evaporated water, leading to relatively stable voltage distribution of single cells in the stack. In addition, the slightly increased fluctuation of voltage distribution of single cells in the stack was observed at the inlet temperature of humidified

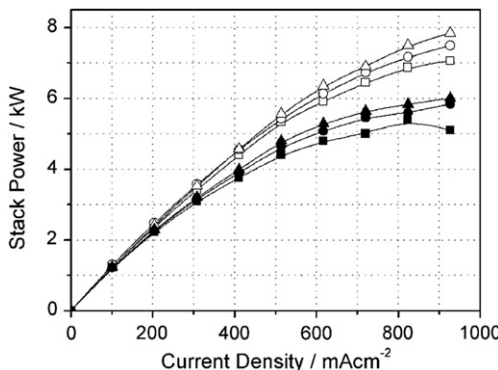


Fig. 6. Output power of the stack at different current density with supply of dry hydrogen (solid) and humidified hydrogen (open) under different inlet gas temperatures: 75 °C (square), 80 °C (circle), and 85 °C (triangle).

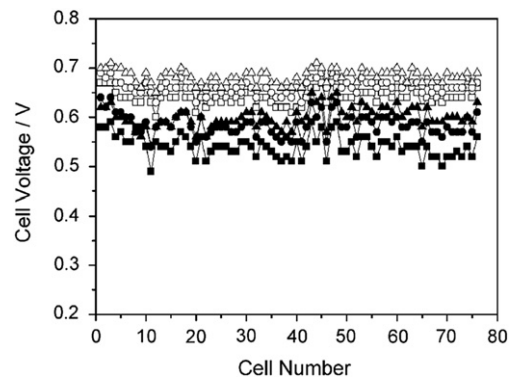


Fig. 7. Voltage distribution of single cells in the assembled stack with supply of dry hydrogen (solid) and humidified hydrogen (open) under different inlet gas temperatures: 75 °C (square), 80 °C (circle), and 85 °C (triangle).

anode gas of 85 °C (corresponded to relative humidity of about 68.4%), probably attributed to the “flooding” phenomenon in some of single cells in the stack. Nevertheless, the uniformity of single cells in the stack was relatively stable when the humidified anode gas was fed to the stack in this experimental range, indicating that the stack can be potentially applied for practical applications at 95 °C.

Average voltage of single cells in the stack at 600 mA cm⁻² was plotted in Fig. 8 as a function of stack temperature under different inlet temperatures of humidified anode gas. When the inlet temperature of humidified anode gas was fixed at 75 °C, the average voltage of single cells in the stack monotonically decreased from 0.667 V to 0.643 V with the increase of stack temperature from 85 °C to 95 °C, attributed to the decrease in water content in the stack. However, peak average voltages of single cells in the stack were observed to be 0.685 V and 0.694 V for the inlet temperature of humidified anode gas of 80 °C and 85 °C, respectively. This non-monotonic behavior in average voltage with the stack temperature probably resulted from the balance between the lack of water induced by evaporation and the increased electrode reaction kinetics in the stack. At the stack temperature below 90 °C, the evaporation of water is less pronounced and the increased electrode reaction kinetics with the increase in stack temperature dominates the performance, leading to the improved performance with the increase in stack temperature. With further increasing stack temperature above 90 °C, the evaporation of water becomes fast and the according increased membrane resistance may

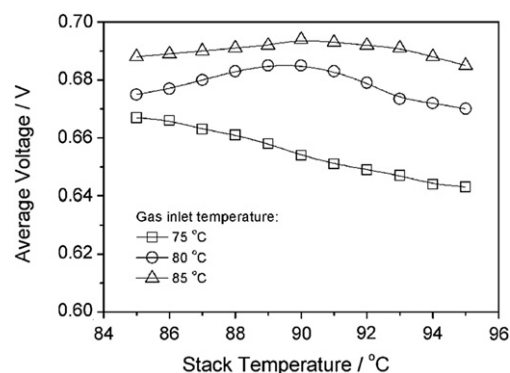


Fig. 8. Instantaneous average voltage of the stack with the supply of humidified hydrogen as a function of stack temperature at different inlet gas temperatures: 75 °C (square), 80 °C (circle), and 85 °C (triangle).

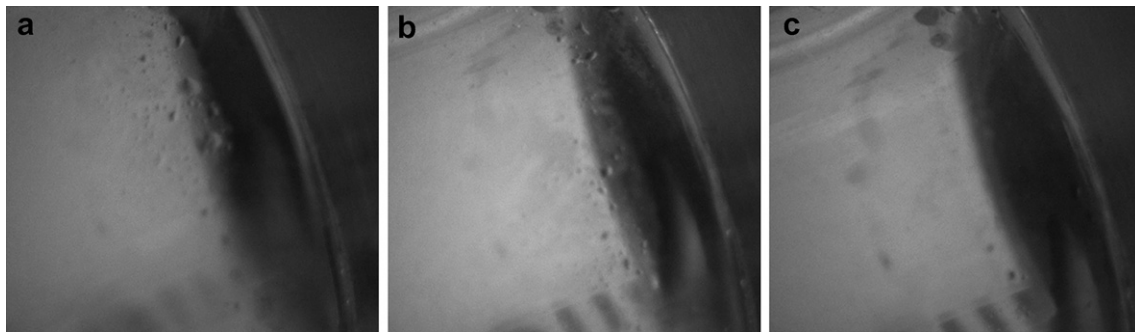


Fig. 9. Water accumulation at cathode outlet of the stack with the supply of dry hydrogen at different operating temperatures: (a) 85 °C, (b) 90 °C, and (c) 95 °C.

dominate the performance of the stack. Accordingly, the performance of the stack decreased with the further increase in stack temperature.

The water accumulation at cathode outlet was monitored with a high-speed camera under different stack temperatures using dry hydrogen and humidified air as reaction gases with the inlet gas temperature of 85 °C to have a better understanding on the temperature-dependent performance of the stack. It can be seen from Fig. 9 that the amount of accumulated water at cathode outlet decreased with the increase in the operating temperature of the stack. At the stack temperatures of 85 °C and 90 °C, the accumulated water was clearly observed, whereas at the stack temperature of 95 °C, no accumulated water was observed at the cathode outlet. This observation suggested that the decrease in stack performance at 95 °C could be attributed to increased resistance of the stack caused by the lack of water in the system. While the stack temperature is below 90 °C, enough water existed in the system and the performance increased with the increase in temperature as the electrode reaction kinetics can be enhanced with the temperature.

It should be noted that the degradation of membrane electrolytes, particularly induced by humidity variation, is one of the major concerns for practical application of PEMFCs [22]. We have previously reported that composite membranes containing Nafion ionomers and ePTFE matrix exhibited enhanced durability compared to pristine Nafion membranes during fuel cell operations at 65 °C under altered relative humidity [17]. It is expected that membranes described in this study may undergo similar trend at elevated temperature. The durability investigation deserves further detailed study.

4. Conclusion

Composite membranes containing ePTFE matrix and short side chain perfluorinated sulfonated ionomers were applied as electrolytes for proton exchange membrane fuel cell applications. It was demonstrated that fuel cells using such composite membranes as electrolytes exhibited reasonable performance at 95 °C under reduced relative humidity, reaching 0.61 V at 800 mA cm⁻² with the testing condition of 95 °C and 40% relative humidity. A 5 kW-class fuel cell stack was assembled using composite membrane as electrolyte and the performance was experimentally evaluated at 95 °C under ambient pressure. The performance exhibits strong dependence on the inlet gas temperature of the stack while operating at 95 °C. With the increase of inlet gas temperature from 75 °C to 85 °C, the stack voltage at 900 mA cm⁻² was enhanced by 11.0% when humidified gases were supplied and it was enhanced by 17.7% when dry hydrogen and humidified air were supplied. In addition, the fluctuation of single cell voltages in the stack is more powerful with the supply of dry hydrogen. Non-monotonic behavior in

average cell voltage with the operating temperature of stack was observed at inlet gas temperature above 80 °C, attributed to the balance between the lack of water induced by evaporation and the increased electrode reaction kinetics in the stack. The results described in this communication demonstrate that fuel cell using ePTFE enhanced short side chain perfluorinated sulfonated ionomer composite membranes has the potential ability working at 95 °C with relative humidity from 40% to 100%, which is a suitable condition for fuel cell vehicle operation in the near term.

Acknowledgments

This work was partially supported by Major State Basic Research Development Program of China “973 Project” (Grant No.: 2012CB215504), the National Science Foundation of China (Grant No.: 51106046), and Self-Determined and Innovative Research Funds of WUT (No.: 2012IV084).

References

- [1] M.C. Williams, Fuel Cell Handbook, 7th ed., EG&G Technical Services Inc., West Virginia, 2004, US Department of Energy.
- [2] S. Srinivasan, Fuel Cells: From Fundamentals to Applications, Springer, Heidelberg, 2006.
- [3] T.E. Lipman, J.L. Edwards, D.M. Kammen, *Energy Pol.* 32 (2004) 101–125.
- [4] Q.F. Li, R.H. He, J.O. Jensen, N.J. Bjerrum, *Chem. Mater.* 15 (2003) 4896–4915.
- [5] J.J. Zhang, Z. Xie, J.L. Zhang, C. Song, T. Navessin, Z. Shi, H.J. Wang, D.P. Wilkinson, Z. Liu, S. Holdcroft, *J. Power Sources* 160 (2006) 872–891.
- [6] M.F. Torchio, M.G. Santarelli, A. Nicali, *J. Power Sources* 149 (2005) 33–43.
- [7] A. Arsalis, M.P. Nielsen, S.K. Kaer, *Int. J. Hydrogen Energy* 37 (2011) 2470–2481.
- [8] L. Barelli, G. Bidini, F. Gallorini, A. Ottaviano, *Appl. Energy* 91 (2012) 13–28.
- [9] E. Quartarone, P. Mustarelli, *Energy Environ. Sci.* 5 (2012) 6436–6444.
- [10] R. Sanderson, S. Abens, J. Hunt, M. Lukas, W. Keil, R. Kopp, G. Steinfeld, D. Hoffman, J. Kuseian, M. Cervi, 2009 Fuel Cell Seminar, Palm Springs, California, Nov. 18 2009.
- [11] F.J. Pinar, P. Canizares, M.A. Rodrigo, D. Ubeda, J. Lobato, *J. Power Sources* 196 (2011) 4306–4313.
- [12] A. Ghelmi, P. Vaccarono, C. Troglia, V. Arcella, *J. Power Sources* 145 (2005) 108–115.
- [13] A.S. Arico, V. Baglio, A. Di Blasi, V. Antonucci, L. Cirillo, A. Ghelmi, V. Arcella, *Desalination* 199 (2006) 271–273.
- [14] A. Stassi, I. Gatto, E. Passalacqua, V. Antonucci, A.S. Arico, L. Merlo, C. Oldani, E. Pagano, *J. Power Sources* 196 (2011) 8925–8930.
- [15] A.S. Arico, A. Di Blasi, G. Brunaccini, F. Sergi, G. Dispenza, L. Andaloro, M. Ferraro, V. Antonucci, P. Asher, S. Buche, D. Fongalland, G.A. Hards, J.D.B. Sharman, A. Bayer, G. Heinz, N. Zandonà, R. Zuber, M. Gebert, M. Corasaniti, A. Ghelmi, D.J. Jones, *Fuel Cells* 10 (2010) 1013–1023.
- [16] C. Gittleman, Automotive Perspective on PEM Evaluation, High Temperature Membrane Working Group Meeting, Washington DC, May 18, 2009.
- [17] H.L. Tang, M. Pan, S.P. Jiang, X. Wang, R.Z. Yuan, *Electrochim. Acta* 52 (2007) 5304–5311.
- [18] H.L. Tang, X.E. Wang, M. Pan, F. Wang, *J. Membr. Sci.* 306 (2007) 298–306.
- [19] H.L. Tang, S.L. Wang, S.P. Jiang, M. Pan, *J. Power Sources* 170 (2007) 140–144.
- [20] Q. Li, C. Xiao, H.N. Zhang, F.T. Chen, P.F. Fang, M. Pan, *J. Power Sources* 196 (2011) 8250–8256.
- [21] M.B. Ji, Z.D. Wei, *Energies* 2 (2009) 1057–1106.
- [22] H.L. Tang, P.K. Shen, S.P. Jiang, F. Wang, M. Pan, *J. Power Sources* 170 (2007) 85–92.